The Egyptian Journal of Remote Sensing and Space Sciences (2015) xxx, xxx–xxx

HOSTED BY

National Authority for Remote Sensing and Space Sciences

The Egyptian Journal of Remote Sensing and Space Sciences

www.elsevier.com/locate/ejrs
www.sciencedirect.com

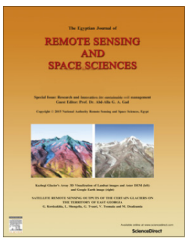

RESEARCH PAPER

# Semi-supervised change detection approach combining sparse fusion and constrained k means for multi-temporal remote sensing images

**Anisha M. Lal** *, **S. Margret Anouncia**

*School of Computing Science and Engineering, VIT University, Vellore, India*

Received 16 April 2015; revised 27 September 2015; accepted 5 October 2015

**KEYWORDS**

Multi-temporal;
Sparse representation;
Constrained k means;
Remote sensing

**Abstract** Change detection is the measure of the thematic change information that can guide to more tangible insights into an underlying process involving land cover, land usage and environmental changes. This paper deals with a semi-supervised change detection approach combining sparse fusion and constrained k means clustering on multi-temporal remote sensing images taken at different timings $T1$ and $T2$. Initially a remote sensing fusion method with sparse representation over learned dictionaries is applied to the difference images. The dictionaries are learned from the difference images adaptively. The fused image is calculated by combining the sparse coefficients and the dictionary. Finally the fused image is subjected to constrained k means (CKM) clustering combining few known labelled patterns and unlabelled patterns which have been collected from experts. The enhanced (CKM) approach (ECKM) is compared with k means, adaptive k means (AKM) and fuzzy c means (FCM). Experimental results were carried out on multi-temporal remote sensing images. Results obtained using PCC and $F1$ measure confirms the effectiveness of the proposed approach. It is also noticed that the ECKM provides better results with less misclassification of errors as compared to k means, adaptive k means and fuzzy c means.



## 1. Introduction

Detection of changes in land cover/land use (Rawat and Kumar, 2015) and changes due to natural hazards is a challenging task to deal with. Semi-supervised change detection techniques are widely used in remote sensing and play an important role in many application domains. They include environmental monitoring (Shalaby and Tateishi, 2007; Ghosh et al., 2015), assessment of land cover dynamics (Rawat et al., 2013), forest monitoring (Kennedy et al., 2007), urban studies (Peijun et al., 2010; Hazarika et al., 2015), etc. The most widely used change detection technique contains three steps, pre-processing, comparison and analysis. In pre-processing, the multispectral images are normalised using band ratio algorithms (Song et al., 2001). The multispectral images are registered, geometric or radiometric corrected,

* Corresponding author. Tel.: +91 8903472011.
E-mail addresses: anishamlal@vit.ac.in (A.M. Lal), smargretanouncia@vit.ac.in (S. Margret Anouncia).

Peer review under responsibility of National Authority for Remote Sensing and Space Sciences.

http://dx.doi.org/10.1016/j.ejrs.2015.10.002
1110-9823 

Please cite this article in press as: Lal, A.M., Margret Anouncia, S., , Semi-supervised change detection approach combining sparse fusion and constrained k means for multi-temporal remote sensing images, Egypt. J. Remote Sensing Space Sci. (2015), http://dx.doi.org/10.1016/j.ejrs.2015.10.002

atmospheric corrected (Hadjimitsis et al., 2010) for further usage in subsequent steps. Comparison of images is done using absolute differencing or change vector analysis for comparing the images taken at different timings. Finally at the analysis phase the changed pixels are differentiated from the unchanged pixels to identify the change (El Bastawesy et al., 2014; El Hattab, 2014).

Based on the literature (Subudhi et al., 2014; Hussain et al., 2013) of sorting out the changed pixels from the unchanged one two approaches are commonly used, supervised and unsupervised. Supervised approach needs to reference map information for setting parameters whereas an unsupervised approach does not. Since a supervised approach (Volpi et al., 2013) provides higher change detection accuracies compared to unsupervised, a reference map is difficult to obtain for certain remote sensing applications. Hence a semi-supervised approach (Lal et al., 2015a; Roy et al., 2012) is proposed with a combination of sparse fusion (Lal et al., 2015b).

The use of semi-supervised and unsupervised approaches has been well documented in the literature (Bovolo et al., 2008). Among them the most widely used is the novel approach using an ensemble of semi-supervised classifiers proposed by Roy et al. (2014) for change detection in remotely sensed images. The approach uses a multiple classifier system in a semi-supervised (learning) framework instead of using a single weak classifier. Iterative learning of base classifiers is continued using the selected unlabelled patterns along with a few labelled patterns. Ensemble agreement is utilised for choosing the unlabelled patterns for the next training step. Finally, each of the unlabelled patterns is assigned to a specific class by fusing the outcome of base classifiers using some combination rule. A novel spatio-contextual fuzzy clustering algorithm was proposed by Subudhi et al. (2014) for unsupervised change detection from multispectral and multi-temporal remote sensing images. The proposed technique uses fuzzy Gibbs Markov Random Field (GMRF) to model the spatial grey level attributes of the multispectral difference image. The change detection problem is solved using the maximum a posteriori probability (MAP) estimation principle. The MAP estimator of the fuzzy GMRF modelled difference image is found to be exponential in nature. Mishra et al. (2012) have used two fuzzy clustering algorithms, namely fuzzy c-means (FCM) and Gustafson–Kessel clustering (GKC) along with local information for unsupervised change detection in multi-temporal remote sensing images. Ghosh et al. (2011) proposed a context-sensitive technique for unsupervised change detection in multi-temporal remote sensing images. The technique is based on a fuzzy clustering approach and takes care of spatial correlation between neighbouring pixels of the difference image produced by comparing two images acquired on the same geographical area at different times.

In this paper a change detection technique for multi-temporal remote sensing images is proposed with four fundamental steps: pre-processing, comparison, fusion and analysis. After comparison the difference images are fused for further analysis in the proposed approach. Based on the literature, (Gong et al., 2012; Lal and Anouncia, 2015) fusion also plays an important role in change detection for remotely sensed images. An improved AIHS (IAIHS) method was proposed for pan sharpening and multi-spectral images by Leung et al. (2014). Through the IAIHS method, the amount of spatial details injected into each band of the multispectral (MS) image is appropriately determined by a weighting matrix, which is defined on the basis of the edges of the panchromatic and MS images and the proportions between the MS bands. An innovative object-oriented change detection approach based on multi-scale fusion was proposed by Wang et al. (2013). This approach introduced the classical colour texture segmentation algorithm J-segmentation (JSEG) to change detection and achieved the multi-scale feature extraction and comparison of objects based on the sequence of J-images produced in JSEG. A novel spatial and spectral fusion model (SASFM) that uses sparse matrix factorization to fuse remote sensing imagery with different spatial and spectral properties has been proposed by Huang et al. (2014).

On the basis of the above mentioned analysis, in the literature no method is available that simultaneously takes advantage of both fusion and semi-supervised clustering approaches for change detection. The main objective of this work is to present robust techniques taking the advantages of sparse fusion and constrained k means clustering for multi-temporal remote sensing images. In this paper we propose a combination of sparse fusion and semi-supervised clustering approach detecting changes for multi-temporal and multi-spectral remote sensing images. In greater detail, the proposed method uses ADM and CVA for generating the difference images obtained from two co-registered and radiometrically corrected multispectral band images acquired over the same geographical area at two different instants of time $T1$ and $T2$. The difference images are fused using sparse representation coefficients and the fused image is clustered as changed (C) and unchanged (UC) pixels by applying CKM. In order to assess the effectiveness of the ECKM, we considered multi-temporal data sets corresponding to the geographical areas of Dead Sea in Israel, and compared the results produced by the proposed approach with unsupervised clustering approaches.

The organisation of this paper is as follows. Section 2 presents an overview of the materials and methods and describes the proposed scheme in detail. In Section 3, experimental results and discussion are described. Performance evaluation of results for change detection are analysed in Section 4. Finally, Section 4 draws the conclusions of this work.

## 2. Materials and methods

### 2.1. Study area

The Dead Sea is located in the Middle East, between Jordan and Israel. It is one of the saltiest lakes in the world. Its shores are located 400 m below the sea level. The Dead Sea is 50 km long and 15 km wide at its widest point and lies between 31.544893 N latitude and 35.484123 E longitude. Its main tributary is the Jordan River which lies in the Jordan Rift Valley. The Dead Sea is fed mainly by the Jordan River, which enters the lake from the north. Due to the large-scale projects done by Israel and Jordan to divert water from the Jordan River for the purpose of irrigation and other water needs, the surface of the Dead Sea has been dropping dangerously for at least the past 50 years. If the shrinkage continues, it is likely that the Dead Sea might disappear completely by 2050. The images of Dead Sea in the year 1984 and 2014 has been acquired by the Landsat 5 and 8 satellites both in October having a time window of acquisition (before/after) of thirty

Please cite this article in press as: Lal, A.M., Margret Anouncia, S., , Semi-supervised change detection approach combining sparse fusion and constrained k means for multi-temporal remote sensing images, Egypt. J. Remote Sensing Space Sci. (2015), http://dx.doi.org/10.1016/j.ejrs.2015.10.002

years and the main aim to show the difference of the coasts of the Dead Sea from 1984 until today. In fact the two images Fig. 4(a) and (b) shows how the lake, especially on the south coast, has suffered a significant reduction in the amount of water over the past thirty years. The marked location in the Fig. 1 shows the exact location of the Dead Sea.

### 2.2. Proposed system

The enhanced constrained k means (ECKM) takes advantage of four main methodologies: (i) creation of difference images using ADM and CVA; (ii) difference image fusion using sparse representation; (iii) semi-supervised clustering using constrained k means; (iv) formation of a change detection map. The proposed approach is shown in the block diagram of Fig. 2,

In the proposed approach, let us consider two coregistered and radiometrically corrected multi-temporal images, acquired over the same geographical area with two different timings $T1$ and $T2$. The two difference images are generated using ADM and CVA techniques. The two difference images are then fused using sparse representation by extracting the patches to form a dictionary. The fused images are then subjected to clustering using CKM. A change formation map is constructed from the clustered image comprising of changed and unchanged pixels. The detailed analysis of the proposed approach is given below.

#### 2.2.1. Creation of difference images

The difference images are created from two multispectral images acquired by the Landsat Thematic Mapper sensor of the Landsat-5 satellite and Landsat Operational Land Imager Sensor of the Landsat-8 satellite in an area of Dead Sea, Israel on October 24, 1984 and October 27, 2014. The band combinations used to create the multispectral images are 3, 2, 1 (R–G–B) and 4, 3, 2 (R–G–B) visible colour which are downloaded from (https://earth.esa.int/web/earth-watching/change-detection/content/-/article/the-dead-sea). The difference

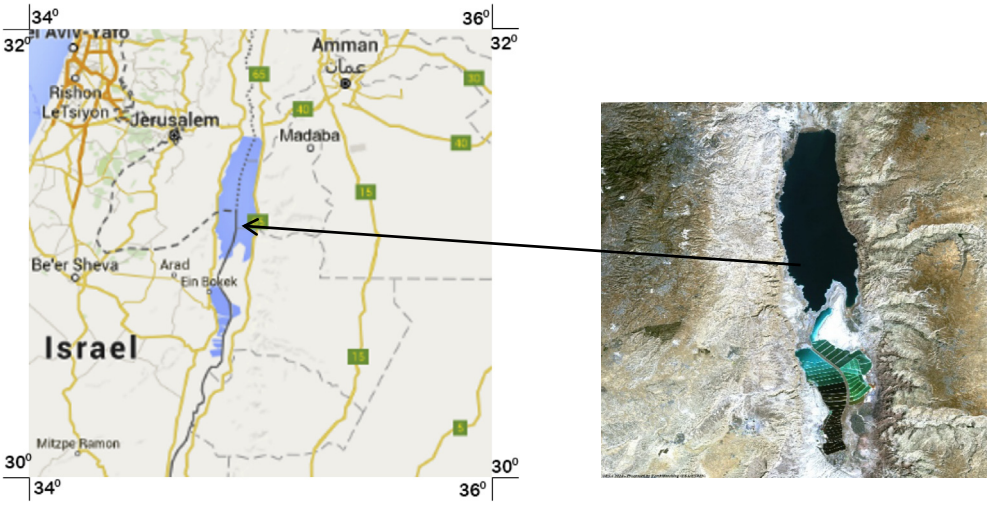


**Figure 1** Map showing the Dead Sea (study area).

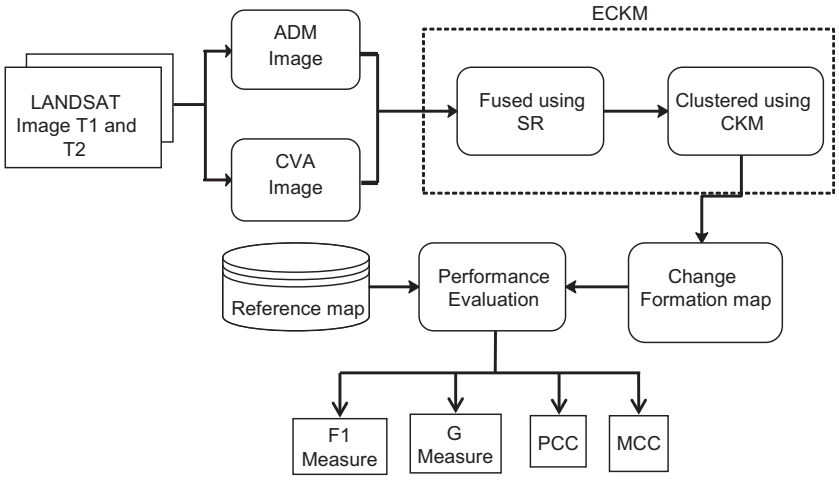


**Figure 2** Proposed system for change detection in remote sensing images.

images are then obtained using ADM and CVA methodologies. The methods are described below.

*2.2.1.1. Absolute difference method (ADM).* The first difference image is created by subtracting the pixel reflectance spectra of the LANDSAT image acquired at time $T1$ and $T2$. The difference image is obtained using absolute differencing which is shown here:

$$Image_{AD} = \sum_{i}^{N} Image_{T1} - Image_{T2}, \quad \text{for } i = 1, 2, \ldots N \tag{1}$$

Here $N$ is the number of bands and the difference image is obtained by subtracting the pixel reflectance of the images. Generally, the higher intensity pixels are considered as changed area and the lower intensity pixels are considered as unchanged area. The threshold value set here is based on the pixel intensity variations of the reference map.

*2.2.1.2. Change vector analysis (CVA) method.* The second difference image is computed by subtracting the spectral change vectors of the LANDSAT image acquired at time $T1$ and $T2$. This technique exploits a simple vector subtraction operator to compare two multispectral images, under analysis, pixel-by-pixel. In some cases, depending on the specific type of changes to be identified, the comparison is made on a subset of the spectral channels. The difference image is computed as the magnitude of spectral change vectors obtained for each pair of corresponding pixels (Ghosh et al., 2009). Let us consider two co-registered and radiometrically corrected $\gamma$ spectral band images $I_{T1}$ and $I_{T2}$, of size $m \times n$, acquired over the same area at different times $T1$ and $T2$, and let DCVA = $\{Image_{CV},\ 1 \leqslant C \leqslant m,\ 1 \leqslant V \leqslant n\}$ be the difference image obtained by applying change vector analysis to $I_{T1}$ and $I_{T2}$,

$$Image_{CV} = \sqrt{\sum_{i=1}^{\gamma} (Image_{CV}(I_{T1}) - Image_{CV}(I_{T2}))^2}$$
$$\text{for } i = 1, 2, \ldots, N \tag{2}$$

Here $Image_{CV}(I_{T1})$ and $Image_{CV}(I_{T2})$ are grey levels at the position $(C, V)$ in the $i$th band of the images $I_{T1}$ and $I_{T2}$. Basically, the change vector analysis uses two channels to map the magnitude of change and the direction of change between the two input images for each date. The length is determined by the vector between two timelines. If there is no change the length will be 0. The direction of the change is interpretable. A threshold value is picked up from the reference image for finding the change. The results achieved by the change vector analysis method are having the capacity to locate and detect the different types of changes in terms of biomass gain and loss (Dubayah et al., 2010).

*2.2.2. Difference images fusion using sparse representation*

In sparse representation image is approximated as a linear combination of a few atoms from the dictionary. The training dictionary contains definite number of overlapped patches mined from observed images. Learned dictionary trained from training patches produce better results to a pre-constructed one. Image signals $x \in R^n$ can be estimated as:

$$x = D \propto \tag{3}$$

where $D \in R^n$ is the dictionary and $\boldsymbol{\alpha}$ is the sparse vector. To obtain a sparse vector which contains the smallest number of non zero elements the following optimization problem is to be solved:

$$\min \| \propto \|_0 \quad \text{such that} \quad \|x - D \propto\|_2^2 \leqslant q \tag{4}$$

where $|| \propto ||_0$ denotes the number of non-zero components in $\alpha$ and $q$ is the approximated error of the input image. The above optimization is an NP-hard problem and can be solved only by a combination of columns. The simplest algorithm to solve this problem is orthogonal matching pursuit (OMP) (Li et al., 2013; Yang and Li, 2012).

**OMP Algorithm**

*The OMP method to compute sparse coefficients for each image,*
$S = \min_{\propto \in R^m} \frac{1}{2} \|x - D \propto\|_2^2$ *such that* $\| \propto \|_0 \leqslant q$
*Step 1: Initialization:* $\alpha = 0$, *residual* $r = x$, *active set* $\Omega = \varnothing$
*Step 2: While* $\| \propto \|_0 < q$
{
*Select the element with maximum correlation with the residual*
$\hat{i} = arg \max_{i=1,2,\ldots m} |d_i^T r|$
*Update the active set, coefficients and residual*
$\Omega = \Omega \cup \hat{i}$
$\propto_\Omega = (d_\Omega^T d_\Omega)^{-1} d_\Omega^T r$
$r = x - d_\Omega \propto_\Omega$
}
*Step 3: End*

In our method, we divide the source images into small patches and use the fixed dictionary D with small size to solve this problem. In addition, a sliding window technique is adopted to make the sparse representation shift invariant, which is of great importance to image fusion. The block diagram of sparse fusion is shown in Fig. 3.

**Sparse Fusion Algorithm**

***Input:*** *Difference images* $DI_i$ *and* $DI_k$
$DI_i$ = *Difference image created using ADM*
$DI_k$ = *Difference image created using CVA*
***Output:*** *Fused image* $DI_f$
***Initialize:*** $q = 0.1$, *block size* $= 8 \times 8$
*Step 1: Load input images* $DI_i$ *and* $DI_k$
*Step 2: Sparse representation using OMP and dictionary,*
$\min \| \propto \|_0$ *such that* $\|x - D \propto\|_2^2 \leqslant q$
*Step 3: Fuse sparse coefficients* $\hat{V}_f$
*Step 4: Restore fused image vectors as,*
$\hat{V}_1 = D\hat{S}_1,\ \hat{V}_2 = D\hat{S}_2, \ldots, \hat{V}_k = D\hat{S}_k$
*Step 5: Reconstruct fused image vector and used fused vectors to reconstruct the image,*
$\hat{V}_f = D\hat{S}_f$
*Step 6: End*
*Finally the fused image is reconstructed from* $\hat{V}_f$

*2.2.3. Fused image clustering using constrained K means*

The fused difference image is clustered using a semi-supervised clustering approach known as constrained k means clustering

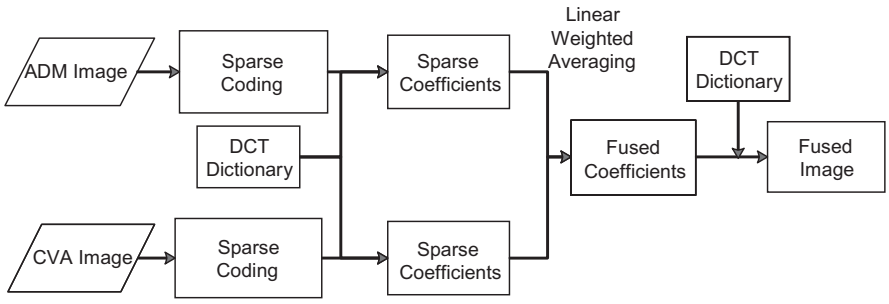


**Figure 3** Block diagram of sparse fusion.

(CKM). This work focuses on the reference map knowledge that can be expressed as a set of instance-level constraints on the clustering process. Here we consider two types of pair-wise constraints, must link constraints (MLC) specify that two instances have to be in the same clusters. Cannot link constraints (CLC) specify that two instances need not be placed in the same cluster. The below algorithm explains the flow of the constraint k means algorithm as given by Wagstaff et al. (2001) for data sets,

**CKM Algorithm**

*Image set I MLC = Clu = ⊆ IxI, CLCClu≠ ⊆ IxI*

1. *Let* $\{C_1 \ldots C_j\}$ *be the initial cluster centres*
2. *For each point* $I_i$ *in I assign it to the closest cluster* $C_i$ *such that violate constraints* ($I_i$, $C_i$, *Clu =, Clu≠*) *is false. If no such cluster exists, fail. return {}.*
3. *For each cluster* $C_k$ *update's its centre by averaging all of the points* $I_j$ *that has been assigned to it.*
4. *Repeat steps 2 and 3 until convergence*
5. *Return* $\{C_1 \ldots C_j\}$

*Violate-constraints (Image I, cluster C, MLC = Clu = ⊆ IxI, CLC = Clu≠ ⊆ IxI)*

1. *For each* $(I; I =) \in Clu =: IfI =\notin C$, *return true*
2. *For each* $(I; I\neq) \in Clu\neq : IfI\neq \in C$, *return true*
3. *Otherwise return false.*

*2.2.4. Formation of the change map*The formation of a change map is mainly used to notify the changed and unchanged areas respectively. Here two cluster centres are obtained by applying CKM clustering denoted by $\gamma_1$ and $\gamma_2$ respectively. Each pixel of the fused image $DI_f$ is assigned to one of the two clusters using the equation given below. Based on the distance of each pixel from the cluster centre, the pixels are assigned to the cluster having a minimum distance. Finally a binary change map is created as given below in:

$$C_{m(x,y)} = \begin{cases} 1, & \|DI_f(x,y) - \gamma_1\| \leqslant \|DI_f(x,y) - \gamma_2\| \\ 0, & \text{otherwise} \end{cases} \quad (5)$$

where $\| \ \|$ is the Euclidean distance. The resultant image contains zeros and ones representing changed and unchanged areas.

## 3. Experimental results and discussion

In order to carry out an experimental analysis aimed at assessing the effectiveness of the proposed approach ECKM, we have considered multi-temporal data sets corresponding to geographical areas of the Dead Sea in Israel. A detailed description of the data set is given below.

### *3.1. Data set related to Dead Sea, Israel area*

The data set used in this experiment is made up of two multispectral images acquired by the Landsat Thematic Mapper sensor of the Landsat-5 satellite in an area of Dead Sea, Israel on October 24, 1984 and October 27, 2014 which is shown in Fig. 4(a) and (b). From the given Landsat image a portion of $512 \times 512$ pixels has been selected for our application. In order to make a quantitative and qualitative evaluation of the effectiveness of the proposed approach, a reference map image shown in Fig. 4(e) was manually defined by experts according to a detailed visual analysis of both the available multi-temporal images and the difference images created by ADM and CVA in Fig. 4 (c) and (d). In the proposed approach the difference images are fused using a sparse representation for further clustering of pixels to changed and unchanged areas. The fused image is shown in Fig. 4(f).

The change detection maps obtained for the Dead Sea data set by the k means, AKM, FCM and CKM without fusion are shown in Fig. 5(a)–(d) and those for, k means, AKM, FCM with fusion and ECKM are shown in Fig. 6(a)–(d) respectively. One can visually compare the change detection maps generated by the existing and ECKM techniques with the corresponding reference image. This gives a rough idea about the quality of the generated change detection maps.

The performance of the proposed approach (ECKM) was analysed both qualitatively as well as quantitatively, the result obtained from the proposed approach was compared with k means, AKM and FCM. It is clear in Fig. 6. that the result achieved by means of proposed approach ECKM seems to be far better than other existing methods visually.

The effectiveness of the proposed change detection approach is evaluated totally by analysing the change detection map. The change detection map obtained by CKM seems to be better than FCM for the Dead Sea data set because the number of unchanged pixels wrongly identified as changed pixels has been generated at larger portions by the FCM. The same inference can be drawn for this data set comparing k means, AKM, and FCM without fusion and with fusion. The observation is similar for our proposed approach; ECKM is doing better than CKM. This leads us to judge the effectiveness of our proposed approach quantitatively, which obviously is better than visual inspection and is presented here.

Please cite this article in press as: Lal, A.M., Margret Anouncia, S., , Semi-supervised change detection approach combining sparse fusion and constrained k means for multi-temporal remote sensing images, Egypt. J. Remote Sensing Space Sci. (2015), http://dx.doi.org/10.1016/j.ejrs.2015.10.002

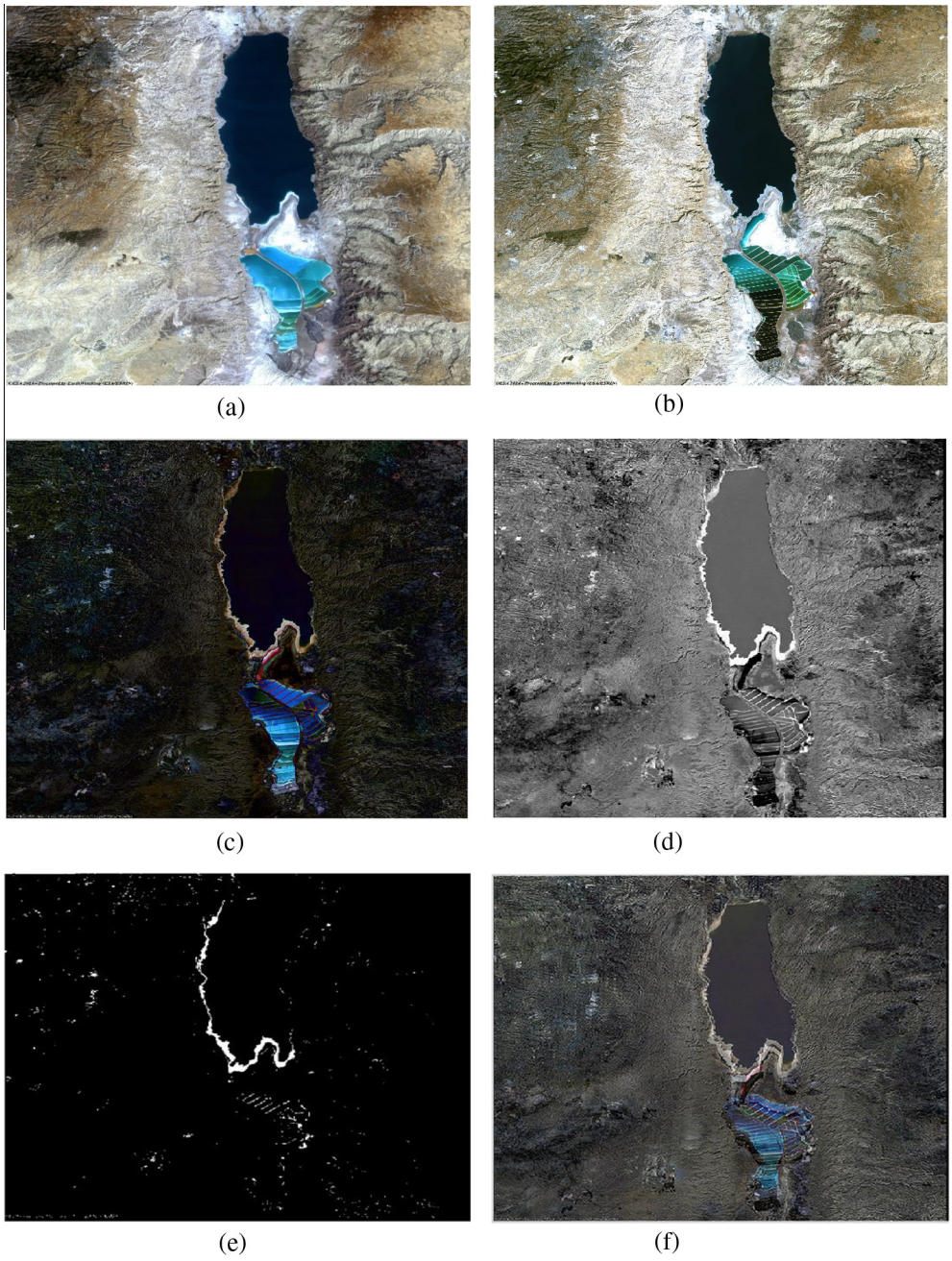


**Figure 4** (a) Landsat 5 image acquired on October 24, 1984. (b) Landsat 8 image acquired on October 27, 2014. (c) Difference image generated using CVA technique. (d) Difference image generated using ADM technique. (e) Reference map of the changed area. (f) Fused image using SR.

## 4. Performance evaluations of results

For the quantitative assessment of the proposed technique, the following quantities suggested by Rosenfield and Fitzpatrick-Lins (1986) have been computed for each change map with respect to the reference map.

*Tp* – the number of changed pixels identified correctly.

*Tn* – the number of pixels correctly identified as unchanged.

*Fn* – the number of changed pixels wrongly identified as unchanged pixels.

*Fp* – the number of unchanged pixels identified as changed pixels.

The quantities given above are evaluated by a confusion matrix and various metrics can be obtained using the above derived quantities to assess the performance of an algorithm. In this paper, the following metrics are adopted:

1. Overall error (OE): Overall error deals with the probability that a changed pixel is wrongly identified as an unchanged pixel.

Please cite this article in press as: Lal, A.M., Margret Anouncia, S., , Semi-supervised change detection approach combining sparse fusion and constrained k means for multi-temporal remote sensing images, Egypt. J. Remote Sensing Space Sci. (2015), http://dx.doi.org/10.1016/j.ejrs.2015.10.002

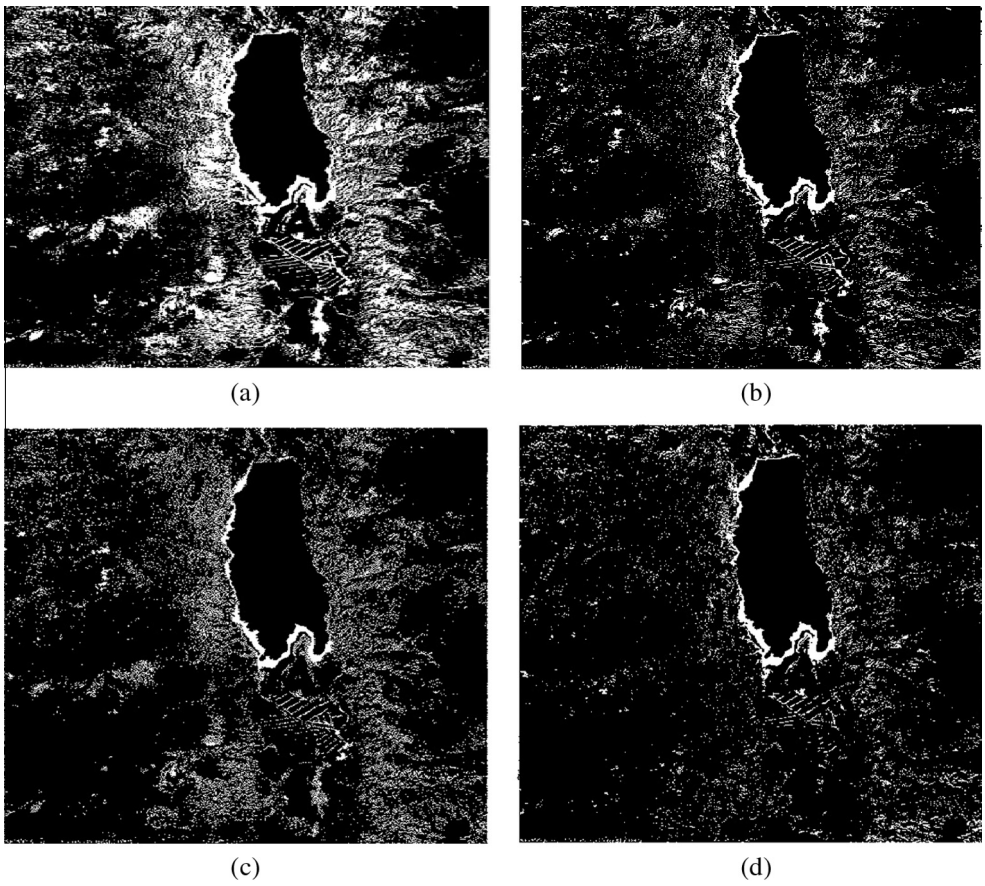


**Figure 5** Change detected via various methods without fusion. (a) Change detected using k means. (b) Change detected using AKM. (c) Change detected using FCM. (d) Change detected using CKM.

$$OE = \frac{Fn}{Fn + Tp} \tag{6}$$

2. Commission error (CE): Commission error deals with the probability that an unchanged pixel is wrongly identified as a changed pixel.

$$CE = \frac{Fp}{Tn + Fp} \tag{7}$$

3. Percentage correct classification (PCC): It identifies the overall accuracy of the proposed method by means of detecting the changed pixels as changed and unchanged pixels as unchanged.

$$PCC = \frac{(Tp + Tn)}{(Tp + Tn + Fp + Fn)} \tag{8}$$

4. Precision: Precision is referred to the fraction of changed pixels identified correctly.

$$Precision = \frac{Tp}{Tp + Fp} \tag{9}$$

5. Recall: Recall is referred to the fraction of changed pixels identified as unchanged.

$$Recall = \frac{Tp}{Tp + Fn} \tag{10}$$

6. $F1$ measure: $F1$ measure is a measure which combines precision and recall. It is a harmonic mean of both.

$$F1measure = 2 * \frac{Precision * Recall}{Precision + Recall} \tag{11}$$

7. $G$ measure: $G$ measure is a geometric mean of precision and recall

$$Gmeasure = \sqrt{precision * recall} \tag{12}$$

8. MCC (Mathew's correlation coefficient)

$$MCC = \frac{Tp * Tn - Fp * Fn}{\sqrt{(Tp + Fp)(Tn + Fn)(Tp + Fn)(Tn + Fp)}} \tag{13}$$

From Tables 1–4 and Figs. 7–10 it's very clear that the proposed approach ECKM has obtained the highest PCC 98.5% among all the existing methods such as k means, AKM and FCM. An analysis has been carried out in terms of OE and CE. It was conveyed that the lesser the value of OE and CE the better is the technique. The overall error (OE) 0.06% obtained in the proposed approach ECKM indicates that changed pixels have been almost identified accurately with less misclassification errors. The CE obtained by the proposed approach is also lesser than the existing techniques. The $F1$ measure obtained by ECKM is 0.65 which is more than k means, AKM and FCM. The other quantitative measures such as recall, precision, $G$ measure and MCC also provides better results for the proposed approach ECKM as shown in Tables 2 and 4 and Figs. 8 and 10. The computational time taken is also less compared to the existing methods.

Please cite this article in press as: Lal, A.M., Margret Anouncia, S., , Semi-supervised change detection approach combining sparse fusion and constrained k means for multi-temporal remote sensing images, Egypt. J. Remote Sensing Space Sci. (2015), http://dx.doi.org/10.1016/j.ejrs.2015.10.002

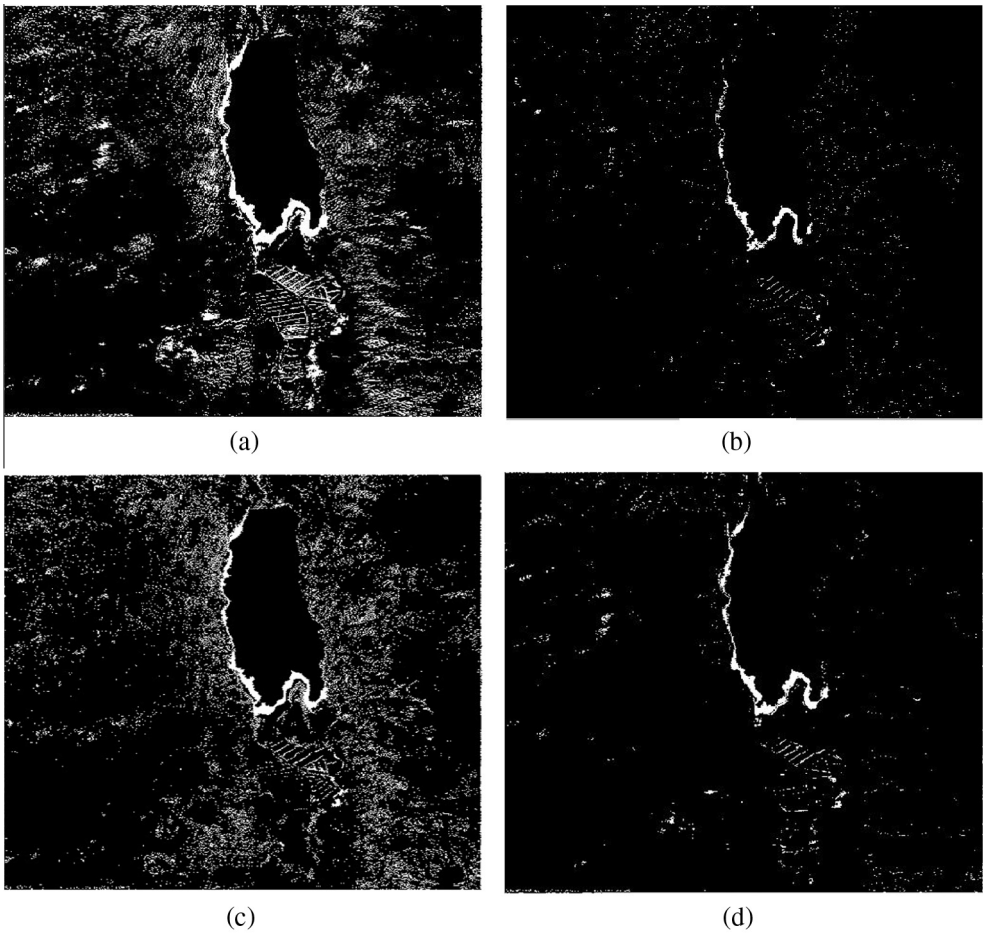


**Figure 6** Change detected via various methods with fusion (a) Change detected using k means. (b) Change detected using AKM. (c) Change detected using FCM. (d) Change detected using ECKM.

**Table 1** Results of various parameters used for quantitative comparison of the existing methods without fusion.

| Method | *Tp* (pixels) | *Tn* (pixels) | *Fp* (pixels) | *Fn* (pixels) | *OE* (%) | *CE* (%) | *PCC* (%) |
|---|---|---|---|---|---|---|---|
| K means | 1779 | 197,683 | 61,460 | 1222 | 40.7 | 23.7 | 76.0 |
| FCM | 2421 | 232,282 | 26,861 | 580 | 19.3 | 10.3 | 89.5 |
| AKM | 2478 | 233,110 | 26,033 | 539 | 17.8 | 10.0 | 89.8 |
| CKM | 2556 | 239,679 | 19,464 | 445 | 14.8 | 7.51 | 92.4 |

**Table 2** Results of various parameters used for quantitative comparison of the existing methods without fusion.

| Method | Precision | Recall | *F*1 measure | *G* measure | MCC |
|---|---|---|---|---|---|
| K means | 0.0281 | 0.5928 | 0.053 | 0.1291 | 3.5168 |
| FCM | 0.0843 | 0.7991 | 0.152 | 0.2596 | 5.5900 |
| AKM | 0.0869 | 0.8213 | 0.157 | 0.2672 | 5.7765 |
| CKM | 0.1161 | 0.8517 | 0.204 | 0.3144 | 6.1262 |

From an overall analysis it is felt that while solving the change detection problem, incorporating fusion of the images with semi-supervised clustering of the output is improved compared to existing ones. The existing techniques require the assumption of distributions of clusters and are very time consuming (k means, AKM, FCM). On the other hand the proposed approach concentrates more on the changed areas to further predict changes in the near future.

**Table 3** Results of various parameters used for quantitative comparison of the existing methods with fusion.

| Method | *Tp* (pixels) | *Tn* (pixels) | *Fp* (pixels) | *Fn* (pixels) | *OE* (%) | *CE* (%) | *PCC* (%) |
|---|---|---|---|---|---|---|---|
| K means | 2390 | 232,730 | 26,413 | 611 | 20.3 | 10.1 | 89.6 |
| FCM | 2791 | 254,204 | 2939 | 210 | 7.00 | 1.91 | 98.0 |
| AKM | 2869 | 255,265 | 3878 | 132 | 4.40 | 1.50 | 98.4 |
| ECKM | 3740 | 254,512 | 3622 | 270 | 0.06 | 0.14 | 98.5 |

Please cite this article in press as: Lal, A.M., Margret Anouncia, S., , Semi-supervised change detection approach combining sparse fusion and constrained k means for multi-temporal remote sensing images, Egypt. J. Remote Sensing Space Sci. (2015), http://dx.doi.org/10.1016/j.ejrs.2015.10.002

**Table 4** Results of various parameters used for quantitative comparison of the existing methods with fusion.

| Method | Precision | Recall | *G* measure | *F*1 measure | MCC |
|---|---|---|---|---|---|
| K means | 0.0830 | 0.7964 | 0.2571 | 0.15 | 5.5622 |
| FCM | 0.3611 | 0.9300 | 0.5795 | 0.52 | 7.0948 |
| AKM | 0.4252 | 0.9560 | 0.6376 | 0.58 | 7.3236 |
| ECKM | 0.5080 | 0.9327 | 0.6883 | 0.65 | 9.5187 |

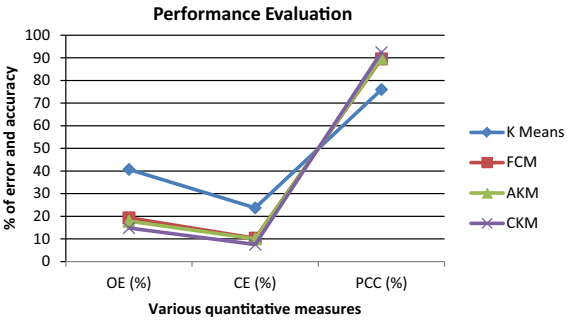


**Figure 7** Performance evaluation of the existing methods without fusion.

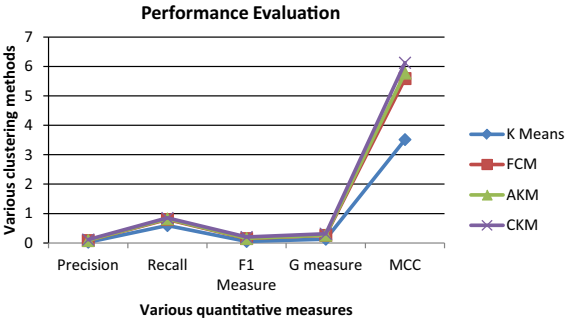


**Figure 8** Quantitative performance evaluation of the existing methods without fusion.

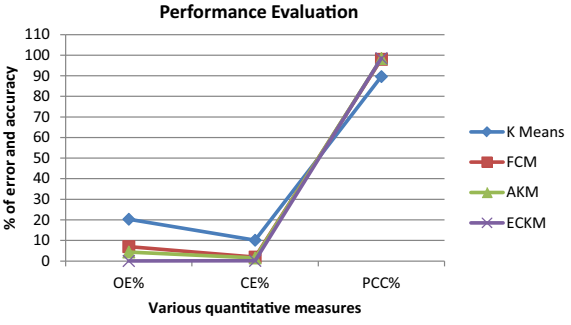


**Figure 9** Performance evaluation of ECKM of the existing methods with fusion.

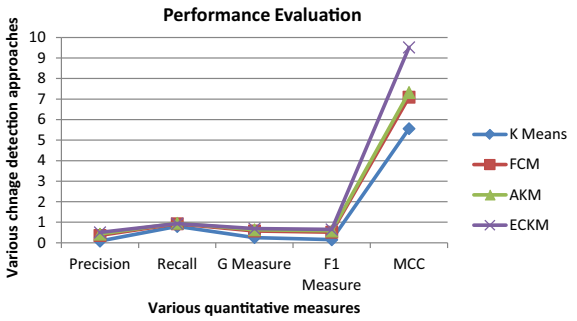


**Figure 10** Quantitative performance evaluation of ECKM of the existing methods with fusion.

## 5. Conclusion

A semi-supervised change detection method combining the idea of sparse fusion and CKM clustering is designed. The devised methodology is applied to the multi-temporal remotely sensed images. A seed point is randomly chosen on the reference image based on the background knowledge of the image. Considering the seed point as a centroid, the fused image is subjected to the clustering process. The formed clusters differentiate the changed region from an unchanged one. To make visibility more, the changed regions are exposed prominently. In order to achieve it, the distances between the clusters with respect to the fused points are computed. Points with minimum distance are assigned as 1 while with the maximum distance is assigned as 0. Due to the conversion of binary points, the region with the change would be highlighted prominently. On comparing the time taken to complete the process, it is noted that the designed ECKM performed considerably faster than other existing methods. Experimental results of the designed process are evaluated for different real multi-temporal data sets and the effectiveness is proved through the results obtained. The results showed a significant accuracy when compared to the other existing methods.

## References

Bovolo, F., Bruzzone, L., Marconcini, M., 2008. A novel approach to unsupervised change detection based on a semi supervised SVM and a similarity measure. IEEE Trans. Geosci. Remote Sens. 46 (7), 2070–2082.

Dubayah, R.O., Sheldon, S.L., Clark, D.B., Hofton, M.A., Blair, J. B., Hurtt, G.C., Chazdon, R.L., 2010. Estimation of tropical forest height and biomass dynamics using lidar remote sensing at La Selva, Costa Rica. J. Geophys. Res.: Biogeosci. (2005–2012) 115 (G2), 1–17.

El Bastawesy, Mohammed, Gabr, Safwat, Mohamed, Ihab., 2014. Assessment of hydrological changes in the Nile River due to the construction of Renaissance Dam in Ethiopia. Egypt. J. Remote Sens. Space Sci. 18, 65–75.

El-Hattab, Mamdouh M., 2014. Change detection and restoration alternatives for the Egyptian Lake Maryut. Egypt. J. Remote Sens. Space Sci. 18, 9–16.

Ghosh, S., Patra, S., Ghosh, A., 2009. An unsupervised context-sensitive change detection technique based on modified

self-organizing feature map neural network. Int. J. Approximate Reasoning 50 (1), 37–50.
Ghosh, A., Mishra, N.S., Ghosh, S., 2011. Fuzzy clustering algorithms for unsupervised change detection in remote sensing images. Inf. Sci. 181 (4), 699–715.
Ghosh, M.K., Kumar, L., Roy, C., 2015. Monitoring the coastline change of Hatiya Island in Bangladesh using remote sensing techniques. ISPRS J. Photogramm. Remote Sens. 101, 137–144.
Gong, M., Zhou, Z., Ma, J., 2012. Change detection in synthetic aperture radar images based on image fusion and fuzzy clustering. IEEE Trans. Image Process. 21 (4), 2141–2151.
Hadjimitsis, D.G., Papadavid, G., Agapiou, A., Themistocleous, K., Hadjimitsis, M.G., Retalis, A., Clayton, C.R.I., 2010. Atmospheric correction for satellite remotely sensed data intended for agricultural applications: impact on vegetation indices. Nat. Hazards Earth Syst. Sci. 10 (1), 89–95.
Hazarika, Nabajit, Das, Apurba Kumar, Borah, Suranjana Bhaswati, 2015. Assessing land-use changes driven by river dynamics in chronically flood affected Upper Brahmaputra plains, India, using RS-GIS techniques. Egypt. J. Remote Sens. Space Sci. 18, 107–118.
Huang, B., Song, H., Cui, H., Peng, J., Xu, Z., 2014. Spatial and spectral image fusion using sparse matrix factorization. IEEE Trans. Geosci. Remote Sens. 52 (3), 1693–1704.
Hussain, M., Chen, D., Cheng, A., Wei, H., Stanley, D., 2013. Change detection from remotely sensed images: from pixel-based to object-based approaches. ISPRS J. Photogramm. Remote Sens. 80, 91–106.
Kennedy, R.E., Cohen, W.B., Schroeder, T.A., 2007. Trajectory-based change detection for automated characterization of forest disturbance dynamics. Remote Sens. Environ. 110 (3), 370–386.
Lal, A.M., Anouncia, S.M., 2015. Detection of boundaries by fusing the topographic sheets and multi-spectral images for geographic landscapes. Int. J. Ecol. Dev.™ 30 (3), 11–25.
Lal, Anisha M., Margret Anouncia, S., Gopalakrishnan, M., 2015a. Multispectral image change revealing using translation invariant wavelet transform fusion and adaptive K-means clustering. Int. J. Appl. Environ. Sci. 10 (2), 681–693.
Lal, A.M., Anouncia, S.M., Kombo, O.H., 2015b. A hybrid approach for fusion combining SWT and sparse representation in multispectral images. Indian J. Sci. Technol. 8 (16).
Leung, Y., Liu, J., Zhang, J., 2014. An improved adaptive intensity–hue–saturation method for the fusion of remote sensing images. Geosci. Remote Sens. Lett., IEEE 11 (5), 985–989.
Li, S., Yin, H., Fang, L., 2013. Remote sensing image fusion via sparse representations over learned dictionaries. IEEE Trans. Geosci. Remote Sens. 51 (9), 4779–4789.
Mishra, N.S., Ghosh, S., Ghosh, A., 2012. Fuzzy clustering algorithms incorporating local information for change detection in remotely sensed images. Appl. Soft Comput. 12 (8), 2683–2692.
Peijun, D.U. et al, 2010. Monitoring urban land cover and vegetation change by multi-temporal remote sensing information. Min. Sci. Technol. (China) 20 (6), 922–932.
Rawat, J.S., Kumar, Manish, 2015. Monitoring land use/cover change using remote sensing and GIS techniques: a case study of Hawalbagh block, district Almora, Uttarakhand, India. Egypt. J. Remote Sens. Space Sci. 18, 77–84.
Rawat, J.S., Biswas, Vivekanand, Kumar, Manish, 2013. Changes in land use/cover using geospatial techniques: a case study of Ramnagar town area, district Nainital, Uttarakhand, India. Egypt. J. Remote Sens. Space Sci. 16 (1), 111–117.
Rosenfield, G.H., Fitzpatrick-Lins, K., 1986. A coefficient of agreement as a measure of thematic classification accuracy. Photogramm. Eng. Remote Sens. 52 (2), 223–227.
Roy, M., Ghosh, S., Ghosh, A., 2012. Search-based semi-supervised clustering algorithms for change detection in remotely sensed images. In: India Conference (INDICON), Annual IEEE, pp. 503–507.
Roy, M., Ghosh, S., Ghosh, A., 2014. A novel approach for change detection of remotely sensed images using semi-supervised multiple classifier system. Inf. Sci. 269, 35–47.
Shalaby, A., Tateishi, R., 2007. Remote sensing and GIS for mapping and monitoring land cover and land-use changes in the Northwestern coastal zone of Egypt. Appl. Geog. 27 (1), 28–41.
Song, C., Woodcock, C.E., Seto, K.C., Lenney, M.P., Macomber, S.A., 2001. Classification and change detection using Landsat TM data: when and how to correct atmospheric effects? Remote Sens. Environ. 75 (2), 230–244.
Subudhi, B.N., Bovolo, F., Ghosh, A., Bruzzone, L., 2014. Spatio-contextual fuzzy clustering with Markov random field model for change detection in remotely sensed images. Opt. Laser Technol. 57, 284–292.
Volpi, M., Tuia, D., Bovolo, F., Kanevski, M., Bruzzone, L., 2013. Supervised change detection in VHR images using contextual information and support vector machines. Int. J. Appl. Earth Obs. Geoinf. 20, 77–85.
Wagstaff, K., Cardie, C., Rogers, S., Schrödl, S., 2001. Constrained k-means clustering with background knowledge. In: ICML, vol. 1, pp. 577–584.
Wang, C., Xu, M., Wang, X., Zheng, S., Ma, Z., 2013. Object-oriented change detection approach for high-resolution remote sensing images based on multiscale fusion. J. Appl. Remote Sens. 7 (1), 073696–073696.
Yang, B., Li, S., 2012. Pixel-level image fusion with simultaneous orthogonal matching pursuit. Inf. Fusion 13 (1), 10–19.

Please cite this article in press as: Lal, A.M., Margret Anouncia, S., , Semi-supervised change detection approach combining sparse fusion and constrained k means for multi-temporal remote sensing images, Egypt. J. Remote Sensing Space Sci. (2015), http://dx.doi.org/10.1016/j.ejrs.2015.10.002